2024 IEEE/RSJ International Conference on Intelligent Robots and Systems (IROS)
October 14-18, 2024. Abu Dhabi, UAE

Integrated Electronic Circuitry for Soft Robots using Multi-Material FDM Printing

Cem Aygül,[1] Ritwik Pandey,[2] Krishram Kothimbakam,[2]
Ceren Yılmaz Akkaya,[3] Pratap M. Rao,[2,3,4] and Markus P. Nemitz[1]

***Abstract*— The integration of electronics into compliant materials is typically complex, cumbersome, and jeopardizes system-level compliance. Using multi-material fused deposition modeling, we introduce a framework in which components of a soft robot and conductive traces are deposited in a single print. Our novel procedure for attaching discrete electronic components to printed conductive traces using toluene solvent ensures reliable electrical connections by significantly reducing contact resistance by over an order of magnitude compared to existing methods. This fabrication pipeline is an additional key component that contributes to the broader objective of establishing a fully automated fabrication process for soft robots with integrated electronics. We demonstrate a complete assembly of a terrestrial soft robot and showcase its resilience against physical impacts.**

I. INTRODUCTION

Soft robots are compliant, adaptable, and impact resistant due to the low Shore hardness of their constituting materials. Soft robots find applications in scenarios that require or benefit from physical interactions, standing in stark contrast to their rigid counterparts.

The majority of soft robots are pneumatically actuated, embedding fluidic actuators in single-material systems [1]–[3], with their control circuits and power sources external to the robot [1], [2], [4]–[6]. As the field advances towards untethered soft robots, incorporating all robot components within soft bodies has become a critical focus [1], [3], [7]. Strategies to achieve highly integrated or *fully self-sufficient* soft robots include using CO_2 cartridges instead of pumps [8], power by combustion [9], [10], or electric actuation schemes such as shape memory alloys or dielectric elastomer actuators [11]–[13]. We introduced the term *self-sufficiency* as a measure for evaluating soft robots by their levels of integration [14].

We believe the emergence of fully autonomous, untethered soft robots requires some degree of silicon-based sensing and control. Researchers have been seeking strategies to integrate electronics into soft robots while maintaining system-level compliance. The inclusion of electronics into soft robots is typically perceived as paradoxical, as rigid electronics seems to challenge the very concept of compliance [2].

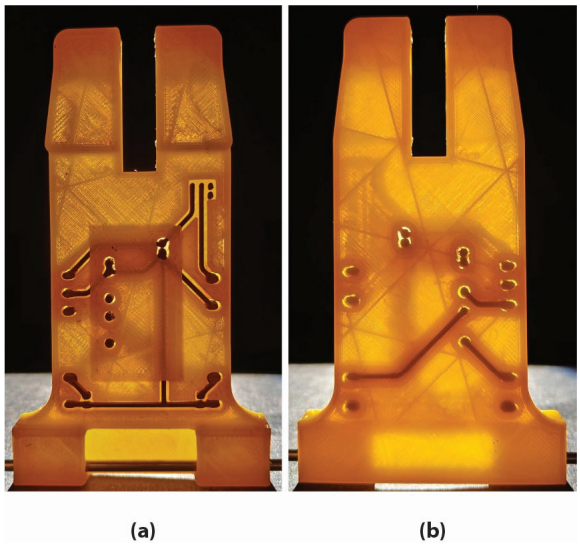

Fig. 1. **Printed robot body with integrated circuitry.** (a) Top and (b) bottom layers of our soft robot. We use a xenon source to highlight the embedded traces within our FDM printed soft robot.

Our previous work demonstrated compromises between elastomeric and rigid components, resulting in soft robots that are increasingly referred to as hybrid systems. Wormbot integrates rigid electronics into elastomeric hulls, preserving system compliance while incorporating silicon-based intelligence [14]. In another study, our quadruped robot combined soft structural elements with conventional electronic components [5]. The electronic components did not obstruct the soft undulation of the robot body; however, integrating soft elastomers with rigid electronics was time-consuming due to many manual fabrication steps.

As an alternative that offers automation, Fused Deposition Modeling (FDM) and conductive filaments can be used for printing components such as antennas [15], inductors [16], RF filters [16], [17], or capacitors [16]. Few examples exist of conductive thermoplastics being used in mobile soft robots. There are examples of printed sensing elements for soft robots [18], [19], but an entire circuitry example is missing. Lazarus et al. used printed conductive traces as a base for selective electroplating improving conductivity and interface characteristics for attaching packaged components [20]. Nassar et al. printed a basic circuit from PLA and a

This work was supported by the National Science Foundation under CAREER Grant No. 2237506.

Corresponding author: Markus P. Nemitz, markus.nemitz@tufts.edu

[1]Faculty of Mechanical Engineering, Tufts University, 419 Boston Ave, Medford, 02155, Massachusetts, United States of America.

[2]Faculty of Robotics Engineering, Worcester Polytechnic Institute, 100 Institute Road, Worcester, 01609, Massachusetts, United States of America.

[3]Faculty of Mechanical and Materials Engineering, Worcester Polytechnic Institute, 100 Institute Road, Worcester, 01609, Massachusetts, United States of America.

[4]Faculty of Chemical Engineering, Worcester Polytechnic Institute, 100 Institute Road, Worcester, 01609, Massachusetts, United States of America.

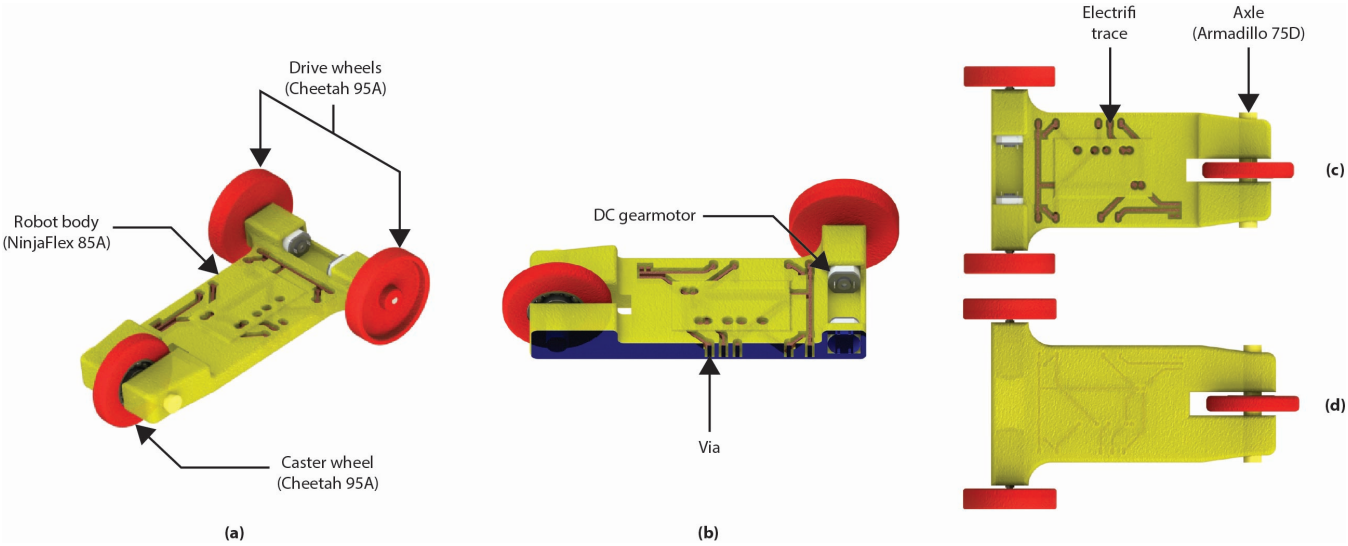

Fig. 2. **A soft wheeled-robot with integrated electronic circuitry.** (a) Isometric view showing the top side of the robot. (b) Cross-sectional side isometric view of vias connecting the top and bottom layers of the printed conductive traces. (c) Top view of the robot, with exposed conductive traces for packaged component attachment. (d) Bottom view of the robot, with the silhouette of bottom layer conductive traces embedded in the TPU matrix. We fabricated the robot using multi-material FDM printing (Figure 5) and demonstrated its soft robotic characteristics: resilience to physical impact including bending and flexing (Figure 9).

conductive thermoplastic but have not applied their strategy to mobile soft robots [21].

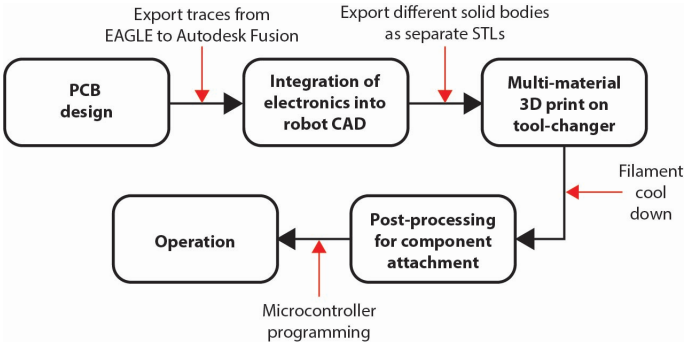

Fig. 3. **The design, fabrication, and operation pipeline for a robot with embedded electronic circuitry.** The flowchart starts with the PCB design, which is moved into a CAD environment for robot integration, followed by 3D printing, post-processing for component attachment, and ultimately robot operation.

In this work, we introduce a methodology for integrating conductive materials into soft robots using *Multi-Material Fused Deposition Modeling (MM-FDM)* (**Figure 1**). We deposit copper-filled conductive polymers and flexible thermoplastic polyurethanes together in a singular print to integrate electronics into soft robotic structures (**Figure 2**). We introduce an attachment methodology that guarantees well-established electrical connections between printed circuitry and electronic components. The methodology does not only eliminate the cumbersome assembly steps for the integration of electronics into the robot body but also helps retain the compliant characteristics of soft robots. We multi-material 3D print a soft car chassis in which we embed the circuitry during a single print job. We showcase the integration of electronic components on the print bed; with minimal manual interventions, we are able to create an operational soft robot with integrated electronics (**Figure 2**).

The contributions of this paper include:

1) The multi-material fused deposition modeling of a soft robot with integrated electronics.
2) The introduction of an attachment methodology that establishes reliable electrical connections between printed circuitry and packaged components.
3) The demonstration of a multi-material, soft car chassis with minimal assembly and fabricated in a single print, surviving physical impacts.

II. Design, Fabrication, and Operation Pipeline

A. Integrated PCB and robot design

To integrate traces into the robot, we start with designing the circuitry in Autodesk EAGLE. In comparison to conventional PCB fabrication, we make alterations to the design rules. We widened the trace widths, increased the clearances between features, and smoothed the curve paths. In our design, we use $1mm$ trace widths and $2mm$ trace thicknesses (i.e., depth). We export the traces as Gerber files; using a converter (FAB3000 by Numerical Innovations), we create two-dimensional STEP files from the Gerber files. Next, we import the STEP files to our CAD environment (**Figure 3**).

In the CAD domain, we are able to extrude the 2D traces into 3D, creating solid bodies. We set the distance between 3D printed layers in accordance with our planned robot dimensions, and extrude vias to connect them at designated points. In our demonstration, we use a two-layered board with a separation layer of $4mm$ thickness.

TABLE I

PRINT PARAMETERS FOR THE DIFFERENT THERMOPLASTICS USED IN FABRICATING THE ROBOT BODY WITH INTEGRATED CIRCUITRY.

Filament	Temperature (°C)	Speed (mm/s)	Tension
NinjaTek Ninjaflex	245	20	Low
NinjaTek Cheetah	235	20	Medium
NinjaTek Armadillo	225	25	High
Multi3D Electrifi	145	10	Medium

Our robot body is printed using NinjaTek NinjaFlex thermoplastic polyurethane (TPU), which has a Shore hardness of 85A at an extrusion temperature of 245°C. The traces are printed from Multi3D Electrifi filament and are printed at a much lower temperature (145°C) than NinjaFlex. We used an E3D tool-changer and a Prusa XL for the prints; four *independent* print heads with direct drive allow for multi-material prints of multiple filaments with different print parameters (**Table I**). As the conductive traces are embedded into the TPU matrix during the print, the print head extruding NinjaFlex comes in contact with the deposited Electrifi traces. In our fabrication trials, this led to the local melting of deposited Electrifi traces, which later adhered to the NinjaFlex nozzle and were spread along its movement path. We hypothesized that this result could lead to short circuits; we introduced gaps between the Electrifi and NinjaFlex regions, effectively mitigating potential printing defects (**Figure 4**).

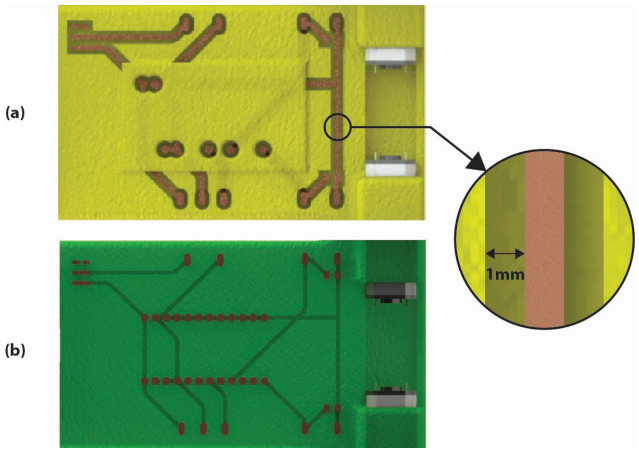

Fig. 4. **Comparison of Electrifi-NinjaFlex interfaces between design iterations.** (a) New design featuring gaps between Electrifi and NinjaFlex sections. (b) Previous design with coincident Electrifi and NinjaFlex sections.

B. Multi-material FDM printing

There are different methodologies to additively manufacture soft materials: Fused Deposition Modeling (FDM), Stereolithography (SLA), and Polyjet printing are among the most commonly used ones. TPUs are commercially available as filament spools usable for FDM, currently featuring Shore hardnesses as low as 60A. The softest materials are available for vat polymerization methods in resin form. These materials can be as soft as 35A, nearing the range of additive curing elastomers. However, due to the printer architecture of SLA, only one resin can reside in the resin tank at a time. Multi-material printing using PolyJet printing can achieve Shore hardnesses as low as 00A [22]; however, despite its promise, PolyJet printing remains prohibitively expensive, with lower-tier, single-material printers starting at approximately $35,000 [23].

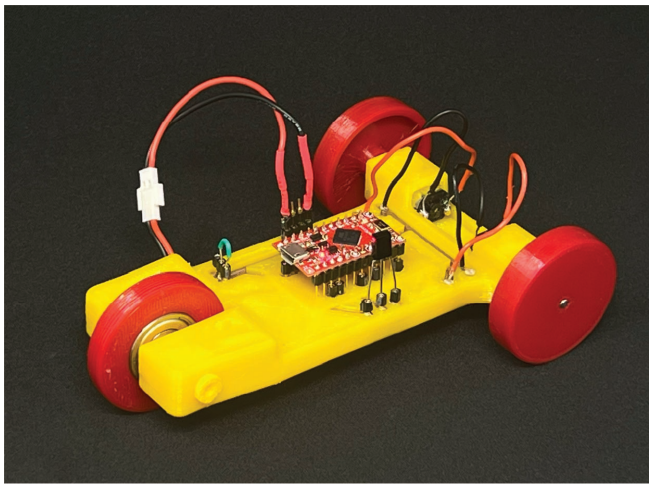

Fig. 5. **The soft wheeled-robot with integrated printed circuitry.** The robot body is made from multiple materials: a TPU structure and copper-filled polymer traces. Separately printed wheels and electronics are assembled to the body to create an operational robot.

FDM printers can be modified for multi-material printing. Modifications include hot-end arrays, selector mechanisms, and splicers. Nonetheless, most of these methods are meant for multi-color printing of rigid materials such as PLA; they typically fail to print TPUs. Elastomeric filaments require constrained filament paths and specific idler tensions, print temperatures, and cooling adjustments depending on their Shore hardness. Therefore, we use a tool-changer, a specialized 3D printer with multiple, *independent* tool heads. We assign different materials to different tool heads, and a selector mechanism picks up the corresponding tool according to the slicer output. This enables us to print different materials on every layer, and embed copper-filled conductive traces into soft TPUs (**Figures 1 and 5**).

We use four extruders on our tool-changer for the fabrication of the soft chassis with integrated traces (**Figure 6**). Two of the extruders deposit the flexible and stretchable filaments NinjaTek Ninjaflex (85A) and NinjaTek Cheetah (95A). The third extruder deposits rigid yet ductile NinjaTek Armadillo (75D), and the fourth extruder deposits Multi3D Electrifi, a composite filament that contains copper particles embedded in a polymer matrix.

C. Electronic component attachment

The attachment of packaged components such as integrated circuits to a printed polymer-conductor matrix poses significant challenges primarily stemming from substantial contact resistances at connector interfaces. In prior studies,

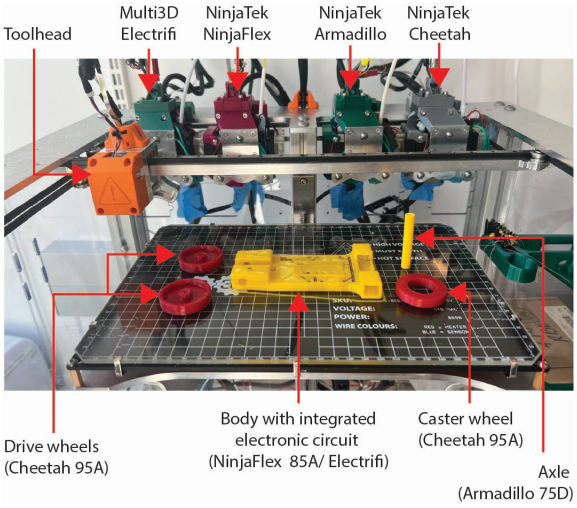

Fig. 6. **Picture of the E3D Toolchanger print bed after the robot is printed.** The robot body with embedded copper-filled traces, two drive wheels, a caster wheel, and an axle are printed in a single job.

researchers have employed the following attachment methods to establish similar connections:

1) **Heat and Plunge:** In this method, the polymer-conductor matrix (comprising a conductive FDM printed trace) or the pads/legs of the electronic component are subjected to heating, followed by the insertion of the component [24].
2) **Silver Paste / Conductive Epoxy:** This approach involves the application of silver paste or conductive epoxy to the contact points, after which the electronic component is positioned. The epoxy is allowed to cure before using the circuit [16], [17], [20], [21], [25], [26].
3) **Hole Insertion:** In this method, the legs of through-hole components are inserted into either pre-printed or drilled holes in the polymer-conductor matrix (conductive FDM printed trace) [16], [20].
4) **Melted Conductive Filament Interface:** A small piece of conductive filament is melted and used as an intermediary between the electronic component and the polymer-conductor matrix (conductive FDM printed trace) [16], [20].

We investigated each of these attachment methods by printing $100mm$ x $2mm$ x $2mm$ Electrifi specimens and attaching breakaway headers at intervals of $30mm$ (**Figure 7**). We quantified the resistance of the conductor-polymer matrix using a 4-terminal probe (Hioki RM3545), $\sim$0.83Ω/cm with a $4mm^2$ cross-sectional area. We used the resistance per unit length to calculate the contact resistance, subtracting the resistance of the polymer-conductor matrix from the 2-terminal resistance measurement.

We observed high contact resistances for the heat and plunge as well as melted filament attachment methods. **Table II** shows the results (contact resistances) of our attachment tests. In contrast, the use of conductive silver epoxy (Chemtronics CircuitWorks CW2460) yielded consistent attachments with lower contact resistances. However, the contact resistances, ranging from 40Ω to 130Ω, still presented a significant concern due to power dissipation. We hypothesized that the elevated contact resistances may be attributed to the polymer coating of the copper micro/nanoparticles within the printed polymer-conductor matrix.

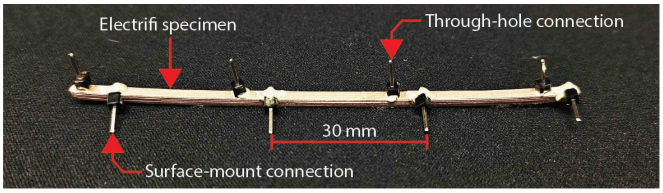

Fig. 7. **Contact resistance test specimen with through-hole and surface-mount attachments.** The attachment points are 30 mm apart and measurements are taken for different attachment methodologies.

We developed a novel attachment method, involving material removal through drilling and the use of a solvent to partially dissolve the polymer matrix and expose the copper infill. The polymer used in Electrifi is a biodegradable polyester. We exposed printed specimens of Electrifi to different solvents, including acetone, 2-methoxyethanol, hexane, dimethylsulfoxide (DMSO), dimethylformamide (DMF), tetrahydrofuran (THF), and toluene, with the objective of assessing the meltability of the polyester. We observed that both THF and toluene were successful in dissolving the polyester. We selected toluene as the preferred solvent due to its comparatively reduced neurotoxic effects in cases of accidental inhalation, lower permeation rate through standard

TABLE II

COMPARISON OF CONTACT RESISTANCES FOR DIFFERENT PACKAGED-COMPONENT ATTACHMENT METHODS.

	Attachment Methods						
Measurement	**Heat & Plunge**	**Melted & Smashed Filament**	**Silver Epoxy**		**Drilling**	**Toulene + Silver Epoxy**	
No.	**Inserted (Ω)**	**Surface (Ω)**	**Surface (Ω)**	**Drilled (Ω)**	**Inserted (Ω)**	**Surface (Ω)**	**Drilled (Ω)**
1	2259997.51	239999997.51	62.51	48.51	3397.51	11.03	10.26
2	2779997.51	153999997.51	84.51	131.51	2667.51	11.78	3.22
3	4749997.51	632.51	70.51	114.49	4557.51	10.08	3.82
4	3099992.53	409.53	40.53	117.53	33992.53	8.21	7.60
5						7.73	3.13
6						8.29	2.74
7						7.07	3.61
8						8.18	5.05
Average	3222496.27	98500259.27	64.52	103.01	11153.77	9.05	4.93
SD (σ)	1075558.18	119033319.90	18.39	37.08	15245.72	1.70	2.66

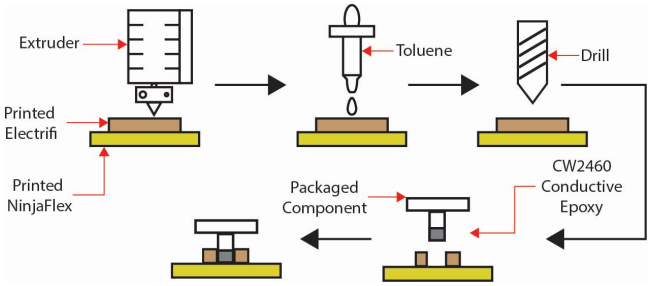

Fig. 8. **Visualization of the packaged component attachment procedure.** Following the printing of copper-filled traces (Multi3D Electrifi), the solvent toluene is used to remove the polymerizing agent, thereby exposing the copper. We remove material at the designated contact point by drilling. We then attach the packaged component to the contact location using conductive epoxy.

nitrile gloves, higher flash point reducing its flammability, and diminished propensity to form explosive peroxides.

We formulated the following attachment process (**Figure 8**):

- FDM print conductive Electrifi traces.
- Add a drop of toluene solvent at the connection point. Excess toluene evaporates into ambient air.
- Drill into or scrape off material at the connection point.
- Add a conductive epoxy (Chemtronics CircuitWorks CW2460) to the contact pad, hole, or the leg/pad of the electronic component.
- Either place the electronic component onto the pad or insert it into the holes.

We evaluated the effectiveness of this attachment method compared to previous attachment test methods, using headers attached 30 mm apart on a $100mm$ x $2mm$ x $2mm$ printed Electrifi specimen (**Figure 7**). The average contact resistance for headers inserted into drilled holes was 4.93Ω, nearly half the resistance of surface-mounted headers, which measured 9.05Ω (Table II). Both results demonstrate a reliable reduction in contact resistance by over an order of magnitude compared to other existing attachment processes.

III. DEMONSTRATION

To demonstrate our fabrication methodology, we 3D-printed a multi-material soft robot with integrated traces. The circuit includes a SparkFun Pro microcontroller, a switch, an IR receiver for remote control, and pads for motor connections (N20 gearmotors). Our design features two layers with vias for interconnections between layers. Upon completion of the fabrication procedure, we programmed the microcontroller in C++; it awaits commands sent via an IR remote, and depending on user input, the robot moves forward, left, or right. To achieve motion, we employ an open-loop controller powering two DC motors. The circuitry does not require power electronics such as MOSFETs or H-bridges; the microcontroller directly applies a control voltage to the motors, and the entire circuit is powered by a USB cable only (**Figure 9 (a), (b), (c)**). Our robot achieved velocities of 0.55 body-lengths per second. Furthermore, we demonstrated the resilience and impact resistance of our robot through deliberate physical interactions including striking, bending, and manipulation (**Figure 9 (d), (e), (f)**).

IV. CONCLUSION AND FUTURE WORK

In this work, we present an integrated design and fabrication strategy for printing both the structure and circuitry of soft mobile robots that use electro-mechanical actuation. Our methodology utilizes easily accessible, off-the-shelf equipment and materials to incorporate soft structural materials and conductive traces into a unified geometry in a single print job, offering new opportunities for the integration of electronics into soft robotic bodies. Using a toolchanger, we deposit multiple materials on the print bed and embed a polymer matrix containing copper particles into a soft, flexible TPU structure. To address the challenges of contact resistance, we introduce a novel post-processing method for attaching packaged components to the printed circuitry. This method involves drilling holes into 3D-printed pads and using a solvent to remove the polymer matrix at the point

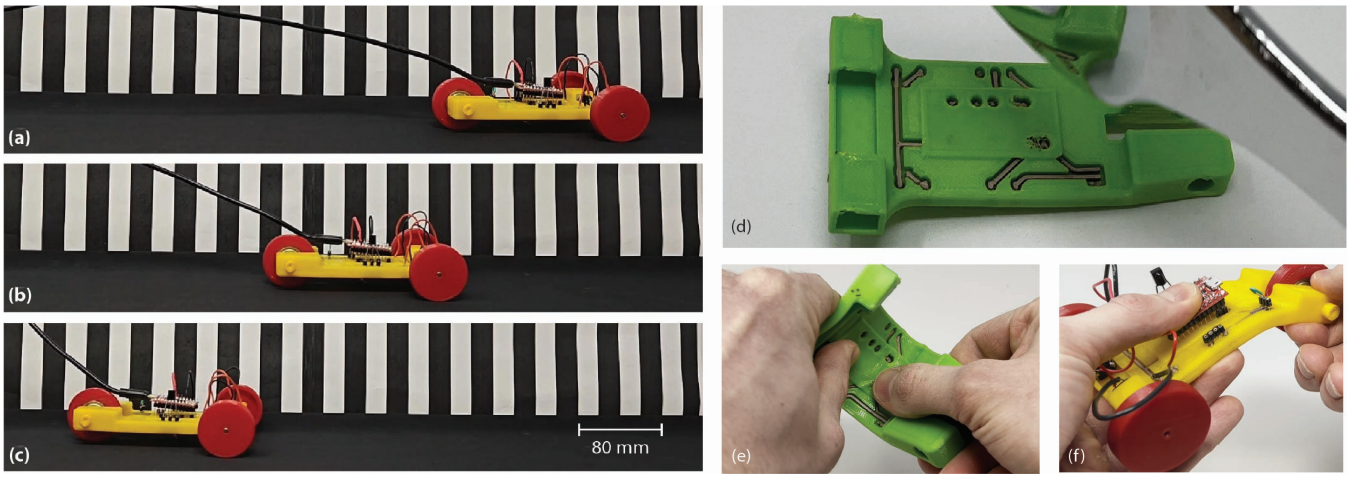

Fig. 9. **Soft wheeled robot demonstrations.** Wheeled soft robot translating uni-axially, powered by a USB cable only. Timestamps at (a) $0s$, (b) $1.6s$, and (c) $3.6s$. (d) Printed robot body with embedded circuitry being impacted by a wrench. (e) Printed robot body with embedded circuitry being bent. (f) Assembled robot body undergoing flexure.

of contact, thereby exposing the copper to establish low-resistance electrical connections. We connect a microcontroller board, an IR receiver, a switch, and two DC motors to control a soft wheeled robot.

For future work, we plan to automate the entire fabrication process by developing unique tool heads for our tool-changer and integrating attachment procedures into the print job. This will involve using different-sized print nozzles to incorporate smaller trace widths, enabling the use of surface mount (SMD) components. We will design new tool heads for drilling, picking-and-placing components, and dispensing solvents and conductive adhesives. We will develop custom G-code scripts to pause the print at specific intervals to insert electronic components and then resume the print to encapsulate the electronics with shock-absorbing TPU.

REFERENCES

[1] C. D. Onal and D. Rus, "Autonomous undulatory serpentine locomotion utilizing body dynamics of a fluidic soft robot," *Bioinspiration & Biomimetics*, vol. 8, no. 2, p. 026003, Mar. 2013, publisher: IOP Publishing.

[2] M. T. Tolley, R. F. Shepherd, B. Mosadegh, K. C. Galloway, M. Wehner, M. Karpelson, R. J. Wood, and G. M. Whitesides, "A Resilient, Untethered Soft Robot," *Soft Robotics*, vol. 1, no. 3, pp. 213–223, Sep. 2014.

[3] D. J. Preston, H. J. Jiang, V. Sanchez, P. Rothemund, J. Rawson, M. P. Nemitz, W.-K. Lee, Z. Suo, C. J. Walsh, and G. M. Whitesides, "A soft ring oscillator," *Science Robotics*, vol. 4, no. 31, p. eaaw5496, Jun. 2019.

[4] N. N. Goldberg, X. Huang, C. Majidi, A. Novelia, O. M. O'Reilly, D. A. Paley, and W. L. Scott, "On Planar Discrete Elastic Rod Models for the Locomotion of Soft Robots," *Soft Robotics*, vol. 6, no. 5, pp. 595–610, Oct. 2019, publisher: Mary Ann Liebert, Inc., publishers.

[5] M. A. Kalın, C. Aygül, A. Türkmen, J. Kwiczak-Yiğitbaşı, B. Baytekin, and O. Özcan, "Design, Fabrication, and Locomotion Analysis of an Untethered Miniature Soft Quadruped, SQuad," *IEEE Robotics and Automation Letters*, vol. 5, no. 3, pp. 3854–3860, Jul. 2020, conference Name: IEEE Robotics and Automation Letters.

[6] T. Duggan, L. Horowitz, A. Ulug, E. Baker, and K. Petersen, "Inchworm-Inspired Locomotion in Untethered Soft Robots," in *2019 2nd IEEE International Conference on Soft Robotics (RoboSoft)*, Apr. 2019, pp. 200–205.

[7] M. M. Coad, L. H. Blumenschein, S. Cutler, J. A. R. Zepeda, N. D. Naclerio, H. El-Hussieny, U. Mehmood, J.-H. Ryu, E. W. Hawkes, and A. M. Okamura, "Vine Robots," *IEEE Robotics & Automation Magazine*, vol. 27, no. 3, pp. 120–132, Sep. 2020, conference Name: IEEE Robotics & Automation Magazine.

[8] K. Bonofiglio, L. Whiteside, M. Angeles, M. Haahr, B. Simpson, J. Palmer, Y. Wu, and M. P. Nemitz, "Soft Fluidic Closed-Loop Controller for Untethered Underwater Gliders," in *2023 IEEE International Conference on Soft Robotics (RoboSoft)*, Apr. 2023, pp. 1–6, iSSN: 2769-4534.

[9] M. Loepfe, C. M. Schumacher, U. B. Lustenberger, and W. J. Stark, "An Untethered, Jumping Roly-Poly Soft Robot Driven by Combustion," *Soft Robotics*, vol. 2, no. 1, pp. 33–41, Mar. 2015, publisher: Mary Ann Liebert, Inc., publishers.

[10] R. F. Shepherd, A. A. Stokes, J. Freake, J. Barber, P. W. Snyder, A. D. Mazzeo, L. Cademartiri, S. A. Morin, and G. M. Whitesides, "Using Explosions to Power a Soft Robot," *Angewandte Chemie International Edition*, vol. 52, no. 10, pp. 2892–2896, 2013, _eprint: https://onlinelibrary.wiley.com/doi/pdf/10.1002/anie.201209540.

[11] C. Laschi, M. Cianchetti, B. Mazzolai, L. Margheri, M. Follador, and P. Dario, "Soft Robot Arm Inspired by the Octopus," *Advanced Robotics*, vol. 26, no. 7, pp. 709–727, Jan. 2012, publisher: Taylor & Francis _eprint: https://doi.org/10.1163/156855312X626343.

[12] H.-T. Lin, G. G. Leisk, and B. Trimmer, "GoQBot: a caterpillar-inspired soft-bodied rolling robot," *Bioinspiration & Biomimetics*, vol. 6, no. 2, p. 026007, Apr. 2011.

[13] M. Duduta, D. R. Clarke, and R. J. Wood, "A high speed soft robot based on dielectric elastomer actuators," in *2017 IEEE International Conference on Robotics and Automation (ICRA)*, May 2017, pp. 4346–4351.

[14] M. P. Nemitz, P. Mihaylov, T. W. Barraclough, D. Ross, and A. A. Stokes, "Using Voice Coils to Actuate Modular Soft Robots: Wormbot, an Example," *Soft Robotics*, vol. 3, no. 4, pp. 198–204, Dec. 2016, publisher: Mary Ann Liebert, Inc., publishers.

[15] M. J. Kim, M. A. Cruz, S. Ye, A. L. Gray, G. L. Smith, N. Lazarus, C. J. Walker, H. H. Sigmarsson, and B. J. Wiley, "One-step electrodeposition of copper on conductive 3D printed objects," *Additive Manufacturing*, vol. 27, pp. 318–326, May 2019.

[16] P. F. Flowers, C. Reyes, S. Ye, M. J. Kim, and B. J. Wiley, "3D printing electronic components and circuits with conductive thermoplastic filament," *Additive Manufacturing*, vol. 18, pp. 156–163, Dec. 2017.

[17] R. Colella, F. P. Chietera, L. Catarinucci, J. F. Salmeron, A. Rivadeneyra, M. A. Carvajal, A. J. Palma, and L. F. Capitán-Vallvey, "Fully 3D-Printed RFID Tags based on Printable Metallic Filament: Performance Comparison with other Fabrication Techniques," in *2019 IEEE-APS Topical Conference on Antennas and Propagation in Wireless Communications (APWC)*, Sep. 2019, pp. 253–257.

[18] S. Mousavi, D. Howard, F. Zhang, J. Leng, and C. H. Wang, "Direct 3D Printing of Highly Anisotropic, Flexible, Constriction-Resistive Sensors for Multidirectional Proprioception in Soft Robots," *ACS Applied Materials & Interfaces*, vol. 12, no. 13, pp. 15 631–15 643, Apr. 2020, publisher: American Chemical Society.

[19] M. Ntagios, P. Escobedo, and R. Dahiya, "3D Printed Robotic Hand with Embedded Touch Sensors," in *2020 IEEE International Conference on Flexible and Printable Sensors and Systems (FLEPS)*, Aug. 2020, pp. 1–4.

[20] N. Lazarus and H. H. Tsang, "3-D Printing Structural Electronics With Conductive Filaments," *IEEE Transactions on Components, Packaging and Manufacturing Technology*, vol. 10, no. 12, pp. 1965–1972, Dec. 2020, conference Name: IEEE Transactions on Components, Packaging and Manufacturing Technology.

[21] H. Nassar and R. Dahiya, "Fused Deposition Modeling-Based 3D-Printed Electrical Interconnects and Circuits," *Advanced Intelligent Systems*, vol. 3, no. 12, p. 2100102, 2021.

[22] L. Severseike, V. Lee, T. Brandon, C. Bakken, and V. Bhatia, "Polyjet 3D printing of tissue-mimicking materials: how well can 3D printed synthetic myocardium replicate mechanical properties of organic myocardium?" Oct. 2019, pages: 825794 Section: New Results.

[23] F. Fischer, "FDM and Polyjet 3D printing," *Popular Plastics & Packaging*, vol. 60, no. 6, pp. 1–7, 2015.

[24] A. R. Jangid, E. B. Strong, J. Chuang, A. W. Martinez, and N. W. Martinez, "Evaluation of commercially-available conductive filaments for 3d printing flexible circuits on paper," *PeerJ Materials Science*, vol. 4, p. e21, 2022.

[25] T. Barši Palmić, J. Slavič, and M. Boltežar, "Process Parameters for FFF 3D-Printed Conductors for Applications in Sensors," *Sensors*, vol. 20, no. 16, p. 4542, Jan. 2020, number: 16 Publisher: Multidisciplinary Digital Publishing Institute.

[26] H. Wolf, D. Mitra, R. Striker, and B. Braaten, "On the Equivalent Circuit Model of a 3D-Printed Conductive Electrifi Transmission Line on a Flexible NinjaFlex Substrate," in *2021 IEEE International Conference on Electro Information Technology (EIT)*, May 2021, pp. 083–085, iSSN: 2154-0373.